ACS Medicinal Chemistry Letters

LETTER

pubs.acs.org/acsmedchemlett

Exploiting the P-1 Pocket of BRCT Domains Toward a Structure Guided Inhibitor Design

Ziyan Yuan,[†] Eric A. Kumar,[†,∥] Stephen J. Campbell,[§,∥] Nicholas Y. Palermo,[†,∥] Smitha Kizhake,[†] J. N. Mark Glover,[§] and Amarnath Natarajan*[,†,‡]

[†]Eppley Institute for Cancer Research, [‡]Departments of Pharmaceutical Sciences, Genetics Cell Biology and Anatomy, University of Nebraska Medical Center, Omaha, Nebraska 68022, United States

[§]Department of Biochemistry, University of Alberta, Edmonton, Alberta T6G 2H7, Canada

Supporting Information

ABSTRACT: Breast cancer gene 1 carboxy terminus (BRCT) domains are found in a number of proteins that are important for DNA damage response (DDR). The BRCT domains bind phosphorylated proteins, and these protein−protein interactions are essential for DDR and DNA repair. High affinity domain specific inhibitors are needed to facilitate the dissection of the protein−protein interactions in the DDR signaling. The BRCT domains of BRCA1 bind phosphorylated protein through a pSXXF consensus recognition motif. We identified a hydrophobic pocket at the P-1 position of the pSXXF binding site. Here we conducted a structure-guided synthesis of peptide analogues with hydrophobic functional groups at the P-1 position. Evaluation of these led to the identification of a peptide mimic **15** with a inhibitory constant (K_i) of 40 nM for BRCT(BRCA1). Analysis of the TopBP1 and MDC1 BRCT domains suggests a similar approach is viable to design high affinity inhibitors.

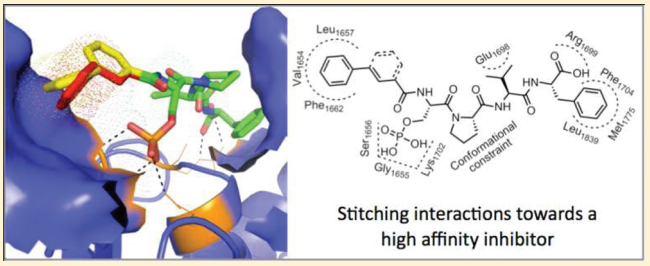

KEYWORDS: Protein−protein interface, peptide mimics, BRCT inhibitors and breast cancer

High affinity small molecule inhibitors of protein−protein interactions (PPIs) are emerging as effective tools to dissect signaling cascades and as potential therapeutics.[1] Tandem carboxy terminus domains of breast cancer gene 1 (BRCT) are considered phosphoprotein binding modules.[2,3] Of particular interest to us are the BRCT domains of the early onset of breast cancer gene 1 (BRCA1). The BRCT-BRCA1 domains recognize and bind phosphorylated proteins such as Abraxas, BACH1, and CtIP.[4−12] PPIs mediated by BRCT-BRCA1 are involved in the regulation of cellular functions such as DNA damage response and repair.[2−14] Mutations in the BRCT-BRCA1 domains are known to alter their binding affinity for peptides derived from their binding partners.[9,15,16] This has been suggested as the molecular basis for predisposing women to breast and ovarian cancers.[2] It is well-known that cancer cells with truncation mutations in the C-terminus of BRCA1 are sensitive to DNA damage based therapeutics, while expression of the wild type BRCA1 in these cells reverses this phenotype.[17−19] Therefore, high affinity BRCT-BRCA1 inhibitors will not only be useful as chemical probes to dissect BRCT-BRCA1 specific signaling but also have the potential to be developed as adjuvants for DNA damage based therapeutics.

Patches and crevices surrounding the hot spot of a PPI can be exploited to enhance the binding of peptide analogues with orthogonal functional groups.[13,20−23] The BRCT-BRCA1 binds tetrapeptides (pSPXF) with micro- to nanomolar affinities.[13,14,24,25] Analysis of BRCT-BRCA1−tetrapeptide structures indicates the presence of a hydrophobic patch formed by Val_{1654}, Leu_{1657}, Pro_{1659}, and Phe_{1662} (VLPF) at the N-terminus of the phosphorylated serine residue (Figure 1).[13,14,26] Here we report a structure-guided synthesis of peptide analogues that occupy the VLPF hydrophobic cluster. Conjugating a phenyl ring with a constrained three-carbon chain through an amide bond to the N-terminus of the phosphoserine residue of the pSPVF peptide resulted in peptide mimics with low nanomolar inhibitory constants (K_i). We conducted a computational study to explore if this strategy will lead to peptide mimics with increased affinity for other BRCT containing proteins (TopBP1 and MDC1). The study suggests that conjugating the hydrophobic fragments to the N-terminus of phosphorylated peptides that bind other BRCT domain containing proteins (TopBP1 and MDC1) may lead to peptide mimics with increased binding affinity.

We used four tetrapeptides (**1**−**4**) and three fluorescent probes (Flu-short, Flu-long, and TMR-long) to determine the optimal probe and an equation to determine K_i values for this, and the K_i values are shown in Table 1. The K_d for the TMR-long probe was ∼3-fold better than that for Flu-long and ∼30-fold better than that for Flu-short. The dissociation constants (K_d) of the fluorescent probes are comparable to those previously reported (Figure S1)[14,24,28,29] We next subjected four unlabeled

Received: June 20, 2011
Accepted: August 17, 2011
Published: August 17, 2011

 © 2011 American Chemical Society

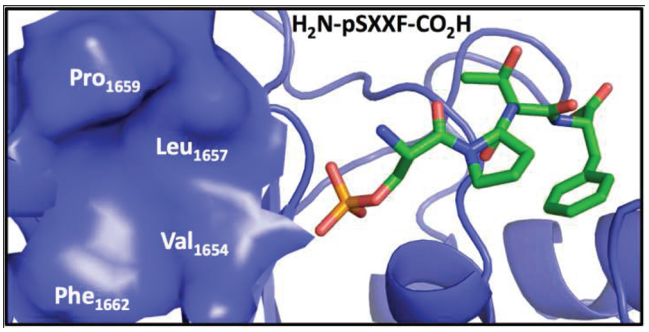

Figure 1. Packing interactions of pSXXF peptide with BRCT-BRCA1 (pdb id: 3K0K). The tetrapeptide and BRCT-BRCA1 are rendered as sticks and cartoon, respectively. The hydrophobic cluster (Val_{1654}, Leu_{1657}, Pro_{1659}, and Phe_{1662}) at the P-1 position is shown as a blue surface. The graphic was generated by Pymol.[27].

peptides (**1**−**4**) to a competition assay with each probe-protein. To determine K_i values, we used six available equations, Cheng−Prussof, Coleska−Wang, Huang, Kenakin, Munson−Rodbard, and Roehrl−Wagner (Table S1).[30−35] The results from these studies suggest that the TMR-long probe and the Coleska−Wang equation were optimal to identify high affinity inhibitors for the BRCT-BRCA1 system (Table S2).

Peptides **5**−**8** with an unnatural amino acid (Nap = napthyl side chain) at the P-1 position were generated to explore the VLPF patch. Peptides **5** and **6** would examine the effect of the stereocenter (*R* and *S*) at the P-1 position while peptide **7** and **8** would determine if the C-terminus of the peptide has an effect on VLPF occupancy. Conjugating the Nap amino acid to the N-terminus of pSPXF peptides results in an increase in the K_i values (μM) when compared to the parent peptides (**5** vs **1** = 1.24 vs 1.85, **7** vs **3** = 0.54 vs 1.96, and **8** vs **4** = 0.13 vs 0.20). Reversal of the stereochemistry from *S* to *R* by incorporating the unnatural Nap amino acid results in ∼15-fold loss of activity (**6** vs **5**). These results suggest that incorporating a hydrophobic group at the P-1 position to occupy the VLPF cluster is an approach that would lead to BRCT-BRCA1 inhibitors with increased affinity.

Next we generated a set of seven peptide mimics (**9**−**15**) with varying functionalities at the P-1 position to determine the optimal linker length, the constraint on the linker, and the size of the hydrophobic group. We observed a decrease in activity with increase in the chain lengths through peptide mimics **9**−**11**, with mimic **9** showing a ∼2-fold higher activity than the parent peptide **4**. Analysis of the K_i values for mimics **9**, **10**, and **11** suggests that the pocket can tolerate no more than a 3 carbon linker. We next explored the size of the VLPF hydrophobic cluster using a napthyl ring and a 3,4-dimethoxy substituted phenyl ring instead of the phenyl ring in mimics **12** and **13**. With these mimics we observed ∼40- and ∼150-fold loss of activity compared to the case of **9**, suggesting that the phenyl ring has the optimal size to occupy the VLPF patch. We next explored if linker flexibility as opposed to linker length is responsible for this change in activity. Mimics **14** and **15** were generated with different levels of linker flexibility. Indeed, we observed increased activity (6−12 fold) in **14** and **15** with restricted linkers compared to **10** (Figure 2). To summarize, this systematic approach resulted in the identification of mimic **15** with a K_i value of 40 nM for BRCT-BRCA1.

Table 1. BRCT-BRCA1 Inhibition (K_i Values)

	R-Group	Peptide	K_i ± SEM (μM)
1	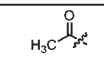	pSPTF-$CONH_2$	1.85 ± 0.06
2		pSPTF-CO_2H	0.27 ± 0.01
3		pSPVF-$CONH_2$	1.96 ± 0.09
4		pSPVF-CO_2H	0.20 ± 0.0
5	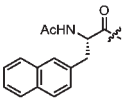	pSPTF-$CONH_2$	1.24 ± 0.04
6	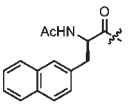	pSPTF-$CONH_2$	19.44 ± 1.91
7	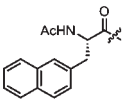	pSPVF-$CONH_2$	0.54 ± 0.03
8	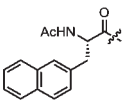	pSPVF-CO_2H	0.13 ± 0.03
9	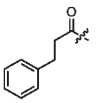	pSPVF-CO_2H	0.10 ± 0.02
10	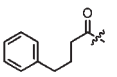	pSPVF-CO_2H	0.50 ± 0.05
11	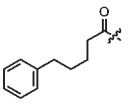	pSPVF-CO_2H	12.05 ± 0.29
12	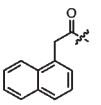	pSPVF-CO_2H	15.67 ± 0.36
13	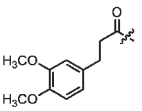	pSPVF-CO_2H	4.04 ± 0.07
14	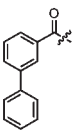	pSPVF-CO_2H	0.08 ± 0.01
15	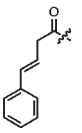	pSPVF-CO_2H	0.04 ± 0.01

We next conducted a hybrid docking molecular dynamics simulation to determine the probable structure and computationally determine the $\Delta\Delta G$ (**14** − **4** and **15** − **4**). The coordinates for peptide **2** bound to BRCT-BRCA1 were obtained from the structure (pdb id: 3K0K) and the hydroxyl on P+2 threonine was replaced with the methyl to generate peptide **4**.

dx.doi.org/10.1021/ml200147a |*ACS Med. Chem. Lett.* 2011, 2, 764–767

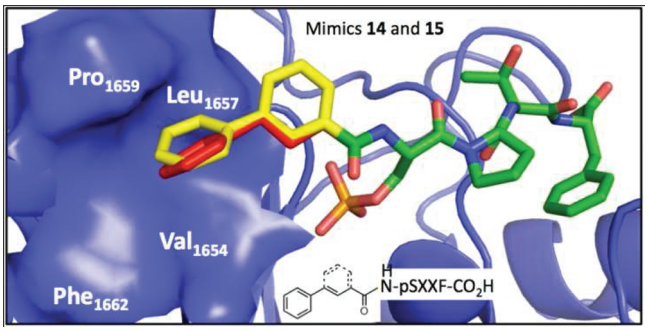

Figure 2. Packing interactions of peptide mimics **14** and **15** with BRCT-BRCA1 (pdb id: 3K0K). The coordinates were derived from a hybrid docking molecular dynamics simulation, and the graphic was generated by Pymol.[27]

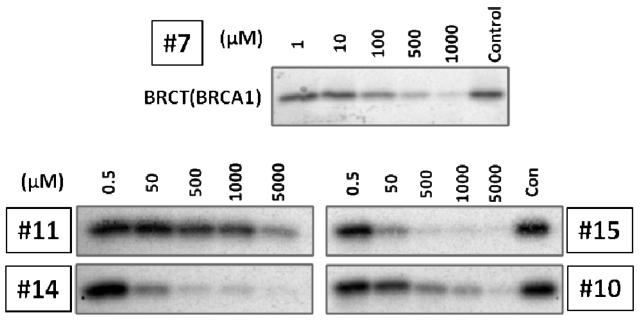

Figure 3. Competitive streptavidin pulldown of the BRCT-BRCA1/BACH1 peptide interaction with peptide mimics (**7**, **10**, **11**, **14**, and **15**). Control indicates binding of the BRCT-BRCA1 to an immobilized phospho BACH1 peptide on streptavidin agarose beads in the presence of vehicle. Titrations are shown with increasing concentration of peptide mimics. The band intensities were quantified using Image-J software, and pulldown IC_{50} values were determined through curve fitting using SigmaPlot.

R groups of peptides (**14** and **15**) were substituted using YASARA.[36] The positions of all atoms of the receptor and the parent peptide residues (pSPVF) were fixed. Water and the simulation box were added using the YASARA "Cell neutralization and pKa prediction" experiment. Each ligand was then refined for 50 ps using the YAMBER force field. The energies of binding were calculated using AutoDock Vina in single calculation mode.[37] The $\Delta\Delta G$ values obtained computationally were 0.4 and 0.9 kcal for **14** and **15**, respectively, and are consistent with the experimental results. We conducted a similar study with pSQEY-BRCT-MDC1 (pdb id: 3K05)[25] and pTPELY-BRCT-TopBP1 (pdb id: 3AL3).[38,39] The $\Delta\Delta G$ values with and without the R groups in **14** and **15** ranged from 0.15 to 0.53 kcal (Table S3). In summary, these studies suggest that exploring crevices and patches adjacent to the hot spots of PPIs is a viable strategy to improve the binding affinity of ligands.

To determine the relative affinities of the peptide mimics for BRCT-BRCA1 in an orthogonal biochemical study, we conducted a competitive streptavidin pulldown study using an *in vitro* transcription translation matrix (Figure 3). BRCT-BRCA1 (1646−1859) was expressed by *in vitro* transcription translation in the presence of 35-S labeled methionine. A mixture of phospho-BACH1 peptide immobilized on streptavidin−agarose beads and peptide mimics was incubated with the BRCT-BRCA1. The beads were then isolated, and the bound protein was subjected to polyacrylamide gel electrophoresis and exposed to phosphor screen. The relative band intensity was quantified by Image-J software, and the pulldown IC_{50} values were determined through curve fitting using SigmaPlot. In summary, the most potent peptide mimics **14** and **15** identified from the FP assay were also the most potent in the *in vitro* transcription translation assay.

In conclusion, analysis of the BRCT−BRCA1−pSXXF complex structures suggested the presence of a hydrophobic cluster (VLPF) at the P-1 position of the pSXXF binding site. A systematic structure guided iterative synthesis and screening of peptide mimics resulted in the identification of BRCT−BRCA1 binders with higher affinity. A constrained 3-carbon linker with a phenyl ring conjugated to the N-terminus of pSPVF peptide results in mimics with low nanomolar K_i values. A systematic analysis of the available equations led to the identification of the Coleska−Wang equation as the optimal model for determining the K_i values for this system. A computational study suggests such an approach can be extended to other BRCT containing proteins (MDC1 and TopBP1). Finally, the potencies of peptide mimics identified in the FP assay correlate with the *in vitro* biochemical data.

■ ASSOCIATED CONTENT

Supporting Information. Experimental methods, Tables S1−S3 (models to determine K_i values, K_i values of **1**−**4**, and computational study to explore the P-1 site on BRCT domains), and Figures S1−S5 (determination of K_i values, LC traces, and mass spectra). This material is available free of charge via the Internet at http://pubs.acs.org.

■ AUTHOR INFORMATION

Corresponding Author

*Phone: (402) 559 3793. Fax: (402) 559 8270. E-mail: anatarajan@unmc.edu.

Author Contributions

‖Equal contribution.

Funding Sources

Funding SourcesThis project was supported in part by NIH T32CA009476 (E.A.K. and N.Y.P.), Alberta Cancer Board—G218000116 (J.N.M.G.), and NIH R01CA127239 (A.N.).

■ ACKNOWLEDGMENT

We would like to thank the UNMC mass spectrometry core facility for MS analysis.

■ ABBREVIATIONS

DDR, DNA damage response; PPI, protein−protein interaction; BRCT, carboxy terminus domains of breast cancer gene 1; BRCA1, breast cancer gene 1

■ REFERENCES

(1) Wells, J. A.; McClendon, C. L. Reaching for high-hanging fruit in drug discovery at protein-protein interfaces. *Nature* **2007**, *450*, 1001–1009.

(2) Manke, I. A.; Lowery, D. M.; Nguyen, A.; Yaffe, M. B. BRCT repeats as phosphopeptide-binding modules involved in protein targeting. *Science* **2003**, *302*, 636–9.
(3) Yu, X.; Chini, C. C.; He, M.; Mer, G.; Chen, J. The BRCT domain is a phospho-protein binding domain. *Science* **2003**, *302*, 639–42.
(4) Kim, H.; Huang, J.; Chen, J. CCDC98 is a BRCA1-BRCT domain-binding protein involved in the DNA damage response. *Nat. Struct. Mol. Biol.* **2007**, *14*, 710–5.
(5) Wang, B.; Matsuoka, S.; Ballif, B. A.; Zhang, D.; Smogorzewska, A.; Gygi, S. P.; Elledge, S. J. Abraxas and RAP80 form a BRCA1 protein complex required for the DNA damage response. *Science* **2007**, *316*, 1194–8.
(6) Cantor, S. B.; Bell, D. W.; Ganesan, S.; Kass, E. M.; Drapkin, R.; Grossman, S.; Wahrer, D. C.; Sgroi, D. C.; Lane, W. S.; Haber, D. A.; Livingston, D. M. BACH1, a novel helicase-like protein, interacts directly with BRCA1 and contributes to its DNA repair function. *Cell* **2001**, *105*, 149–60.
(7) Varma, A. K.; Brown, R. S.; Birrane, G.; Ladias, J. A. Structural basis for cell cycle checkpoint control by the BRCA1-CtIP complex. *Biochemistry* **2005**, *44*, 10941–6.
(8) Williams, R. S.; Green, R.; Glover, J. N. Crystal structure of the BRCT repeat region from the breast cancer-associated protein BRCA1. *Nat. Struct. Biol.* **2001**, *8*, 838–842.
(9) Williams, R. S.; Glover, J. N. Structural consequences of a cancer-causing BRCA1-BRCT missense mutation. *J. Biol. Chem.* **2003**, *278*, 2630–2635.
(10) Williams, R. S.; Lee, M. S.; Hau, D. D.; Glover, J. N. Structural basis of phosphopeptide recognition by the BRCT domain of BRCA1. *Nat. Struct. Mol. Biol.* **2004**, *11*, 519–25.
(11) Yu, X.; Chen, J. DNA damage-induced cell cycle checkpoint control requires CtIP, a phosphorylation-dependent binding partner of BRCA1 C-terminal domains. *Mol. Cell. Biol.* **2004**, *24*, 9478–86.
(12) Callebaut, I.; Mornon, J. P. From BRCA1 to RAP1: a widespread BRCT module closely associated with DNA repair. *FEBS Lett.* **1997**, *400*, 25–30.
(13) Joseph, P. R.; Yuan, Z.; Kumar, E. A.; Lokesh, G. L.; Kizhake, S.; Rajarathnam, K.; Natarajan, A. Structural characterization of BRCT−tetrapeptide binding interactions. *Biochem. Biophys. Res. Commun.* **2010**, *393*, 207–10.
(14) Lokesh, G. L.; Muralidhara, B. K.; Negi, S. S.; Natarajan, A. Thermodynamics of phosphopeptide tethering to BRCT: the structural minima for inhibitor design. *J. Am. Chem. Soc.* **2007**, *129*, 10658–9.
(15) Coquelle, N.; Green, R.; Glover, J. N. Impact of BRCA1 BRCT Domain Missense Substitutions on Phosphopeptide Recognition. *Biochemistry* **2011**, *50*, 4579–4589.
(16) Williams, R. S.; Chasman, D. I.; Hau, D. D.; Hui, B.; Lau, A. Y.; Glover, J. N. Detection of protein folding defects caused by BRCA1-BRCT truncation and missense mutations. *J. Biol. Chem.* **2003**, *278*, 53007–53016.
(17) Thompson, M. E. BRCA1 16 years later: nuclear import and export processes. *FEBS J.* **2010**, *277*, 3072–3078.
(18) Kennedy, R. D.; Quinn, J. E.; Mullan, P. B.; Johnston, P. G.; Harkin, D. P. The role of BRCA1 in the cellular response to chemotherapy. *J. Natl. Cancer Inst.* **2004**, *96*, 1659–68.
(19) Quinn, J. E.; Kennedy, R. D.; Mullan, P. B.; Gilmore, P. M.; Carty, M.; Johnston, P. G.; Harkin, D. P. BRCA1 functions as a differential modulator of chemotherapy-induced apoptosis. *Cancer Res.* **2003**, *63*, 6221–6228.
(20) Arkin, M. R.; Wells, J. A. Small-molecule inhibitors of protein-protein interactions: progressing towards the dream. *Nat. Rev. Drug Discov.* **2004**, *3*, 301–17.
(21) Blazer, L. L.; Neubig, R. R. Small molecule protein-protein interaction inhibitors as CNS therapeutic agents: current progress and future hurdles. *Neuropsychopharmacology* **2009**, *34*, 126–141.
(22) Pagliaro, L.; Felding, J.; Audouze, K.; Nielsen, S. J.; Terry, R. B.; Krog-Jensen, C.; Butcher, S. Emerging classes of protein-protein interaction inhibitors and new tools for their development. *Curr. Opin. Chem. Biol.* **2004**, *8*, 442–449.
(23) Shakespeare, W. C. SH2 domain inhibition: a problem solved? *Curr. Opin. Chem. Biol.* **2001**, *5*, 409–415.
(24) Yuan, Z.; Kumar, E. A.; Kizhake, S.; Natarajan, A. Structure-Activity Relationship Studies To Probe the Phosphoprotein Binding Site on the Carboxy Terminal Domains of the Breast Cancer Susceptibility Gene 1. *J. Med. Chem.* **2011**, *54*, 4264–4268.
(25) Campbell, S. J.; Edwards, R. A.; Glover, J. N. Comparison of the structures and peptide binding specificities of the BRCT domains of MDC1 and BRCA1. *Structure* **2010**, *18*, 167–176.
(26) Shiozaki, E. N.; Gu, L.; Yan, N.; Shi, Y. Structure of the BRCT repeats of BRCA1 bound to a BACH1 phosphopeptide: implications for signaling. *Mol. Cell* **2004**, *14*, 405–12.
(27) Warren, L. *DeLano PyMOL User's Guide*; 2004.
(28) Lokesh, G. L.; Rachamallu, A.; Kumar, G. D.; Natarajan, A. High-throughput fluorescence polarization assay to identify small molecule inhibitors of BRCT domains of breast cancer gene 1. *Anal. Biochem.* **2006**, *352*, 135–41.
(29) Simeonov, A.; Yasgar, A.; Jadhav, A.; Lokesh, G. L.; Klumpp, C.; Michael, S.; Austin, C. P.; Natarajan, A.; Inglese, J. Dual-fluorophore quantitative high-throughput screen for inhibitors of BRCT−phosphoprotein interaction. *Anal. Biochem.* **2008**, *375*, 60–70.
(30) Nikolovska-Coleska, Z.; Wang, R.; Fang, X.; Pan, H.; Tomita, Y.; Li, P.; Roller, P. P.; Krajewski, K.; Saito, N. G.; Stuckey, J. A.; Wang, S. Development and optimization of a binding assay for the XIAP BIR3 domain using fluorescence polarization. *Anal. Biochem.* **2004**, *332*, 261–273.
(31) Cheng, Y.; Prusoff, W. H. Relationship between the inhibition constant (K1) and the concentration of inhibitor which causes 50% inhibition (I50) of an enzymatic reaction. *Biochem. Pharmacol.* **1973**, *22*, 3099–3108.
(32) Kenakin, T. *Pharmacological Analysis of Drug-Receptor Interaction*; Lippincott-Raven: Philadelphia, PA, 1997.
(33) Huang, X. Fluorescence polarization competition assay: the range of resolvable inhibitor potency is limited by the affinity of the fluorescent ligand. *J. Biomol. Screen.* **2003**, *8*, 34–38.
(34) Munson, P. J.; Rodbard, D. An exact correction to the "Cheng-Prusoff" correction. *J. Recept. Res.* **1988**, *8*, 533–546.
(35) Roehrl, M. H.; Wang, J. Y.; Wagner, G. A general framework for development and data analysis of competitive high-throughput screens for small-molecule inhibitors of protein−protein interactions by fluorescence polarization. *Biochemistry* **2004**, *43*, 16056–16066.
(36) Krieger, E.; Darden, T.; Nabuurs, S. B.; Finkelstein, A.; Vriend, G. Making optimal use of empirical energy functions: force-field parameterization in crystal space. *Proteins* **2004**, *57*, 678–683.
(37) Trott, O.; Olson, A. J. AutoDock Vina: improving the speed and accuracy of docking with a new scoring function, efficient optimization, and multithreading. *J. Comput. Chem.* **2010**, *31*, 455–461.
(38) Wang, J.; Gong, Z.; Chen, J. MDC1 collaborates with TopBP1 in DNA replication checkpoint control. *J. Cell Biol.* **2011**, *193*, 267–273.
(39) Leung, C. C.; Gong, Z.; Chen, J.; Glover, J. N. Molecular basis of BACH1/FANCJ recognition by TopBP1 in DNA replication checkpoint control. *J. Biol. Chem.* **2011**, *286*, 4292–4301.